Computational Study of Near-Limit Propagation of Detonation in Hydrogen-Air Mixtures

S. Yungster and K. Radhakrishnan
Institute for Computational Mechanics in Propulsion, Cleveland, Ohio

Since its founding, NASA has been dedicated to the advancement of aeronautics and space science. The NASA Scientific and Technical Information (STI) Program Office plays a key part in helping NASA maintain this important role.

The NASA STI Program Office is operated by Langley Research Center, the Lead Center for NASA's scientific and technical information. The NASA STI Program Office provides access to the NASA STI Database, the largest collection of aeronautical and space science STI in the world. The Program Office is also NASA's institutional mechanism for disseminating the results of its research and development activities. These results are published by NASA in the NASA STI Report Series, which includes the following report types:

- TECHNICAL PUBLICATION. Reports of completed research or a major significant phase of research that present the results of NASA programs and include extensive data or theoretical analysis. Includes compilations of significant scientific and technical data and information deemed to be of continuing reference value. NASA's counterpart of peer-reviewed formal professional papers but has less stringent limitations on manuscript length and extent of graphic presentations.

- TECHNICAL MEMORANDUM. Scientific and technical findings that are preliminary or of specialized interest, e.g., quick release reports, working papers, and bibliographies that contain minimal annotation. Does not contain extensive analysis.

- CONTRACTOR REPORT. Scientific and technical findings by NASA-sponsored contractors and grantees.

- CONFERENCE PUBLICATION. Collected papers from scientific and technical conferences, symposia, seminars, or other meetings sponsored or cosponsored by NASA.

- SPECIAL PUBLICATION. Scientific, technical, or historical information from NASA programs, projects, and missions, often concerned with subjects having substantial public interest.

- TECHNICAL TRANSLATION. English-language translations of foreign scientific and technical material pertinent to NASA's mission.

Specialized services that complement the STI Program Office's diverse offerings include creating custom thesauri, building customized databases, organizing and publishing research results . . . even providing videos.

For more information about the NASA STI Program Office, see the following:

- Access the NASA STI Program Home Page at *http://www.sti.nasa.gov*

- E-mail your question via the Internet to help@sti.nasa.gov

- Fax your question to the NASA Access Help Desk at 301–621–0134

- Telephone the NASA Access Help Desk at 301–621–0390

- Write to:
  NASA Access Help Desk
  NASA Center for AeroSpace Information
  7121 Standard Drive
  Hanover, MD 21076

Computational Study of Near-Limit Propagation of Detonation in Hydrogen-Air Mixtures

S. Yungster and K. Radhakrishnan
Institute for Computational Mechanics in Propulsion, Cleveland, Ohio

National Aeronautics and
Space Administration

Glenn Research Center

October 2002

Available from

COMPUTATIONAL STUDY OF NEAR-LIMIT PROPAGATION OF DETONATION IN HYDROGEN-AIR MIXTURES

S. Yungster and K. Radhakrishnan
Institute for Computational Mechanics in Propulsion
Brook Park, Ohio 44142

Abstract

A computational investigation of the near-limit propagation of detonation in lean and rich hydrogen-air mixtures is presented. The calculations were carried out over an equivalence ratio range of 0.4-5.0, pressures ranging from 0.2 bar to 1.0 bar, and ambient initial temperature. The computations involved solution of the one-dimensional Euler equations with detailed finite-rate chemistry. The numerical method is based on a second-order spatially accurate total-variation-diminishing (TVD) scheme, and a point implicit, first-order-accurate, time marching algorithm. The hydrogen-air combustion was modeled with a 9-species, 19-step reaction mechanism. A multi-level, dynamically adaptive grid was utilized in order to resolve the structure of the detonation. The results of the computations indicate that when hydrogen concentrations are reduced below certain levels, the detonation wave switches from a high-frequency, low amplitude oscillation mode to a low frequency mode exhibiting large fluctuations in the detonation wave speed; that is, a "galloping" propagation mode is established.

Introduction

Recent experimental and computational results indicate that the specific impulse obtained in a hydrogen fueled, air-breathing pulsed detonation engine (PDE) is highest when it is operated under fuel lean conditions[1-3]. However, when the fuel-air equivalence ratio, ϕ, reached values below approximately 0.6, a sharp drop off in thrust and specific impulse was observed experimentally, possibly due to having exceeded the detonability limits for hydrogen-air mixtures.

At fuel-rich conditions, the performance of an air-breathing PDE is significantly degraded. Nevertheless, a potential application of a fuel-rich pulsed detonation rocket engine (PDRE) has been proposed in combination with an ejector. In such a PDRE-ejector engine, the excess fuel in the PDRE tube is mixed and burned with entrained air and subsequently expanded through a nozzle in an unsteady version of the ejector-ramjet concept[4]. Unsteady ejectors are potentially more efficient than their steady-state counterparts[5].

There is therefore considerable practical interest in investigating the limits of detonability for both rich and lean mixtures. Published work on detonability limits is not extensive. Gordon et al.[6] carried out experiments in hydrogen-oxygen

mixtures with different diluents. Of particular interest to the present study are their results for hydrogen-air mixtures which exhibited large oscillations in detonation speed near the detonability limits. Dupre et al.[7] also showed that in hydrogen-air mixtures large detonation velocity fluctuations were obtained when hydrogen concentrations were lowered below a certain level. Because of the large variation in propagation speed, these marginal detonations are sometimes called "galloping" detonations.

Belles[8] suggested that the detonability limits in hydrogen-air and hydrogen-oxygen systems are the mixture compositions for which the conditions at the von Neumann spike lie outside the isothermal branched-chain explosion limits. Belles' analysis included only four chemical reactions. Dove and Tribbeck[9] extended the work of Belles by considering a more complete combustion mechanism. They showed that secondary reactions involving HO_2 cannot be ignored, and that the effects of exothermicity are also important and can lead to a "chain-thermal" explosion. That is, explosions can occur for compositions significantly outside the isothermal limit. However, the numerical methods needed for solving the stiff ODE's describing the combustion process were not sufficiently developed at the time, and they could not determine the boundaries outside the isothermal limits for which explosive behavior would still exist.

In this paper, we investigate first the combustion of hydrogen-air mixtures at the von Neumann spike conditions using the LSENS code[10,11]. Subsequently, we examine in more detail the structure and stability of the detonation wave for near-limit mixtures by conducting one-dimensional computational fluid dynamic (CFD) calculations.

Reaction Kinetics at the von Neumann Spike

The reaction rate equations were integrated under the assumption of a Zeldovich, von Neumann, Doring (ZND) detonation. The actual calculation consisted of two parts:

(i) The determination of the state at the von Neumann spike, which is used as the initial condition for the chemical kinetic calculation. This state was found using the CEA equilibrium code[12].

(ii) The integration of the chemical kinetic rate equations with the initial conditions found in step one. These calcula-

tions were carried out using the LSENS chemical kinetics code[11].

The combustion mechanism used in the calculations in part (ii) and in the CFD computations described later, is based on Jachimowski's model[13], and is listed in Table 1. It consists of 19 elementary reversible reactions among 8 reacting species, with N_2 treated as an inert (i.e., nonreacting) species.

Results are presented in figs. 1 and 2 in the form of ignition delay times as a function of mixture equivalence ratio for two different initial fill pressures: $p_0 = 0.4$ bar and $p_0 = 1.0$ bar. Here, the ignition delay is arbitrarily defined as the time required to increase the temperature of the gas by 25 K. For $p_0 = 0.4$ bar (fig. 1), ignition occurs within a few microseconds for the equivalence ratio range $0.6 < \phi < 3.0$. Outside this range, the ignition delay increases very rapidly. For $p_0 = 1.0$ bar (figure 2), a similar trend is observed, but the curves are significantly steeper on the lean and rich sides of stoichiometric than those at the lower pressure. Also, the ignition delay times near stoichiometric conditions are smaller at the higher pressure. At $\phi = 1$, for example, the ignition delay is 0.83 μs for $p_0 = 0.4$ bar, and 0.36 μs for $p_0 = 1.0$ bar. Figure 2 also includes the value of the detonability limits computed by Belles[8] as well as experimental values obtained by Laffitte[14], as reported in ref. 8.

It is clear from figs. 1 and 2 that the limits of detonability are probably determined by the steep increase in the ignition delay time for very lean and rich mixtures. That is, for mixtures significantly away from stoichiometric conditions, the large ignition delay times may prevent the coupling between the reaction front and the shock wave needed to form a stable detonation wave. Based on this argument, it appears from figs. 1 and 2 that the limits of detonability become further apart as the pressure is lowered, a result also predicted by Belles[8]. This somewhat counterintuitive behavior can be explained from the variation of the ignition delay (or explosion limit) with pressure for hydrogen-air mixtures. Table 2 gives ignition delay times for a stoichiometric hydrogen-air mixture at an initial temperature of 1250 K. It is observed that the ignition delay time is not a monotonic function of pressure. For pressures between 10 and 40 bars, the ignition delay actually increases with pressure.

The precise value of the maximum ignition delay that would allow the establishment of a stable detonation, or the changes in the structure and stability of a detonation wave at near-limit conditions cannot be determined from these type of calculations. To answer these questions a more detailed analysis, based on CFD computations that include the dynamics of the flow and combustion process (and their interaction) is needed. Such analysis is presented in the following sections.

CFD Simulations

As a first step in understanding the behavior of detonation waves at near-limit conditions, we carried out one-dimensional CFD computations. It is well known that detonation waves have a three-dimensional structure, and therefore, a one-dimensional analysis will not be able to investigate the effect of transverse waves. However, such a study will be able to examine, in a relatively quick and inexpensive way (particularly when a detailed reaction model is used to describe the chemistry) the longitudinal stability characteristics of detonation waves. Moreover, a one-dimensional analysis can serve as a basis for subsequent multi-dimensional calculations.

Since detonation limits are not dependent on transport phenomena[6], we neglect all dissipation effects and therefore based our study on the Euler equations. We use the conservation form of the unsteady Euler equations and replace the global continuity equation with the 9 species conservation equations. A detailed description of the set of differential equations and additional state and constitutive equations needed for system closure are given in ref. 15.

The numerical method used for solving the governing equation set is based on Yee's second-order spatially accurate total-variation-diminishing (TVD) scheme[16], and a point implicit, first-order time-accurate marching algorithm. This method is a subset of a more general class of BDF methods considered by Yungster and Radhakrishnan[17]. It is obtained by setting the variables γ=0 and β=1 in equation 4 of ref. 17, and treating only the chemical source term implicitly. Further details about the numerical algorithm are given in ref. 17.

In order to maintain adequate numerical resolution of the detonation wave front, without the need to use hundreds of thousands of grid points, a multi-level, dynamically adaptive grid is utilized. Figure 3 shows a section of the grid at three different times as the detonation wave moves from left to right. The grid constantly adapts to keep the detonation front within the finest grid level. An arbitrary number of levels can be specified. Nine or ten grid levels were used in the present study, and 100 points were included in the finest grid level.

CFD Results

There are two ways in which a detonation can be formed in general: (1) by direct initiation, in which a strong shock wave is generated in the tube (with a charge of solid explosive or by using a high pressure reservoir) and (2) by transition from a deflagration. In this paper, we consider only

development of detonations with direct initiation. Figure 4 shows a schematic of the initiation process used in the present study. A high pressure, high temperature driver gas, consisting of nitrogen, was used in a small region next to the head-end of the tube. As the computation is started, a shock wave travels to the right and an expansion wave propagates to the left, towards the head-end. The shock wave is strong enough to initiate chemical reactions in the combustible mixture. Depending on the mixture properties, the shock wave and the combustion front can subsequently merge and form a detonation wave. The value of the driver pressure, p_{driv}, will determine the degree of overdrive of the resulting detonation wave. The degree of overdrive f is defined as

$$f = D^2 / D_{CJ}^2$$

where D is the actual detonation propagation speed, and D_{CJ} is the theoretical Chapman-Jouguet detonation speed.

The first case considers a stoichiometric mixture of hydrogen-air at $p_0 = 0.4$ bar and $T_0 = 298$ K and a driver pressure ratio, $r_p = p_{driv}/p_0$, of 100. A grid refinement study for this case is presented in figure 5. Numerical results are presented for four successively refined grids having a minimum spacing, Δx_{min}, indicated in each figure. The plots show the variation in the detonation speed with time. Initially the shock wave travels at a constant speed (determined by the initial conditions) slightly above 1500 m/s. Chemical reactions behind the shock front start generating strong compression waves (i.e., a reaction shock) after approximately 10 μs . The reaction shock overtakes the shock front at around 13 μs, strengthening it and sharply increasing its propagation speed (figs. 5b-5d). Subsequently, the detonation wave speed decreases gradually.

It can be observed that the structure of the detonation wave changes with grid spacing. On the coarsest grid (fig. 5a), the detonation reaches a steady propagation speed of $D = 2020$ m/s after the initial transient phase. For the next finer grid (fig. 5b) the computed low frequency oscillation appears to be a numerical artifact. With the finest two grids used in this study (figs 5c and 5d), the detonation reaches a high-frequency, low-amplitude propagation mode; however, with the third grid (fig. 5c) a low frequency mode can still be observed (in addition to the high-frequency one). The solution in Fig. 5d has an average propagation speed of $D = 2025$ m/s, nearly identical to the steady solution in fig. 5a. The frequency of the oscillations, ω, in fig. 5d is 0.90 ± 0.05 MHz.

Figure 6 shows pressure distributions at different times for the grid spacing corresponding to fig. 5d. At $t = 10.8$ μs, chemical reactions behind the shock front have produced a sharp peak in pressure. No change in the shock front propagation speeds occurs at this time. At $t = 13.7$ μs, the reaction shock has overtaken the shock front resulting in a spike in

pressure and propagation speed. After approximately $t = 38.3$ μs, high frequency pressure oscillations become evident downstream of the detonation front.

The theoretical Chapman-Jouguet detonation speed for this mixture, as computed from the chemical equilibrium code CEA[12] is $D_{CJ} = 1956.2$ m/s. Therefore, the results presented in figs. 5 and 6 are actually those of an overdriven detonation, with a degree of overdrive $f = 1.07$. The frequency of oscillation computed in fig. 5d is in close agreement with the results of Sussman[18], who obtained a frequency of 1 MHz on a similar piston-driven detonation computation for a degree of overdrive of $f = 1.1$, slightly higher than that considered here.

In the ballistic range experiments of Lehr[19], which consisted of spherical projectiles being fired into hydrogen-air mixtures, a frequency of oscillation of 1.04 MHz was obtained for a projectile speed of 2029 m/s, and for the same mixture considered in Fig. 5, but at a slightly higher pressure (0.42 bar).

The high-frequency mode of oscillation can be explained by the McVey-Toong wave interaction mechanism[20]. Two fundamental processes form the basis of this mechanism: (i) when a new reaction front is created, compression waves (reaction shocks) are generated that travel upstream and downstream from the new reaction front; (ii) when an old reaction front is extinguished, it must be accompanied by the generation of upstream and downstream rarefaction waves which have a strength comparable to the reaction shocks. The interaction between these waves and the shock front produces the high frequency oscillations, as described in detail in refs. 20 and 17.

To verify that the high-frequency oscillations computed in this case are described by this mechanism, the history of pressure and density in the region immediately behind the detonation front have been plotted in an x-t diagram in fig. 7. This figure shows three pulses corresponding to three oscillation cycles. (The "staircase" appearance of this plot is due to the periodic sliding of the grid to keep track of the detonation front). Careful examination of this figure reveals all of the elements of the McVey-Toong mechanism.

Unless otherwise stated, all subsequent calculations presented below, were carried out on the same grid used in fig. 5d. Figure 8 shows plots of detonation speed as a function of time for several lean mixtures. For $\phi = 0.8$, the structure of the detonation is very similar to that observed in the stoichiometric case, except that the frequency has decreased to 0.76 MHz. For $\phi = 0.6$, the frequency decreases further to 0.52 MHz and an additional low frequency mode appears. At $\phi = 0.5$ the low and high frequency modes are present simultaneously, and at $\phi = 0.4$ the detonation wave almost completely switches from a high-frequency, low-amplitude

oscillation mode to a low-frequency, high-amplitude one; that is, a "galloping" propagation mode is established.

While there is no generally accepted criterion for defining limit behavior, galloping detonations represent the lowest propagation mode of detonation in a tube, and it has been suggested that the detonability limit should be based on the onset of the galloping mode[7].

Figure 9 presents the maximum pressure behind the shock front as a function of time for the same hydrogen-air mixtures as above. This figure shows the increase in the amplitude of the oscillations and the switch to the low frequency mode as the fuel-air equivalence ratio is lowered.

Figure 10 shows the variation in detonation wave speed with time for rich mixtures. Note that as ϕ increases, the frequency of oscillation decreases and the time it takes for the detonation to develop also increases significantly. For $\phi = 4.0$, only a few oscillation cycles were captured before the detonation wave reached the end of the computational domain. The frequencies of oscillation are: 0.62 MHz for $\phi = 2.0$, 0.41 MHz for $\phi = 3.0$, and 0.29 MHz for $\phi = 4.0$.

Pressure effect

The effect of pressure on detonation wave structure was examined and the results are presented in figs. 11 and 12, for $p_0 = 0.2$ and 1.0 bar respectively.

The theoretical Chapman-Jouguet detonation speed for a stoichiometric hydrogen-air mixture at $p_0 = 0.2$ bar and $T_0 = 298$ K is 1939.5 m/s. The average detonation speed computed in fig. 11a after 150 μs is 1960.7 m/s, corresponding to a degree of overdrive of $f = 1.02$.(Note that this calculation used a driver pressure ratio of $r_p = 70$).

The structure of the detonation wave is similar to that for the $p_0 = 0.4$ bar case, but the frequencies of oscillation are much smaller. For $\phi = 1.0$, the frequency is 0.34 ± 0.02 MHz, and it decreases to 0.29 MHz for $\phi = 0.8$. At $\phi = 0.6$, the high frequency oscillations are much less uniform and range from approximately 0.18 MHz to 0.28 MHz. At this equivalence ratio ($\phi = 0.6$) the low frequency mode begins to become evident. At $\phi = 0.4$, the only mode present is the low-frequency one, except during maximum detonation speed when very weak traces of the high frequency mode can be seen.

The results for $p_0 = 1.0$ bar are shown in fig. 12. A finer grid, having a minimum spacing of $\Delta x_{min}=7.324 \times 10^{-5}$ cm, was used in this case, due to the shorter ignition delay times at this pressure near stoichiometric conditions. The theoretical Chapman-Jouguet detonation speed for a stoichiometric hydrogen-air mixture at $p_0 = 1.0$ bar and $T_0 = 298$ K is 1976.7 m/s. The average detonation speed computed in fig.

12a after 15 μs is 2127.7 m/s, corresponding to a degree of overdrive of $f = 1.16$. Note that this calculation used a driver pressure ratio of $r_p = 150$. In general, the higher the pressure, the higher the degree of overdrive needed to obtain the high-frequency, low amplitude mode of oscillation described by the McVey-Toong mechanism.

The results for $p_0 = 1.0$ bar show more variation in the amplitude of oscillation than the $p_0 = 0.4$ and 0.2 bar cases, even though the degree of overdrive is higher in this case. The frequencies of oscillation are also much higher at $p_0 = 1.0$ bar. For the $\phi = 1.0$ case, the frequency of oscillation is 3.2 ± 0.2 MHz. At lower equivalence ratios, the frequencies are 2.71 MHz for $\phi = 0.8$, 2.08 MHz for $\phi = 0.6$, and 1.28 MHz for $\phi = 0.4$. Note that due to the high degree of overdrive, the high-frequency mode persists at the smallest value of the equivalence ratio ($\phi = 0.4$).

Driver pressure ratio effect

The effect of driver pressure ratio, r_p, was investigated for hydrogen-air mixtures at $p_0 = 0.4$ bar. Figure 13 shows the detonation speed for four mixtures at a driver pressure $r_p = 150$. It can be seen that compared with the results of fig. 8, (which were obtained with $r_p = 100$) the oscillations are much more uniform, and have a lower amplitude and a higher frequency. The high-frequency mode is present even for the $\phi = 0.4$ case.

At $\phi=1.0$, the average detonation speed after 50 μs is 2087.3 m/s, corresponding to a degree of overdrive $f = 1.14$. The frequency of oscillation for this case is 1.19 ± 0.03 MHz. The frequencies for the other cases are: 1.09 MHz for $\phi=0.8$, 0.91 MHz for $\phi=0.6$, and 0.63 MHz for $\phi=0.4$.

Figure 14 shows the results for the same mixtures, but a driver pressure ratio of $r_p = 40$. Previous "steady" detonation calculations[3,4] (i.e. coarse-grid computations) using this driver pressure ratio, have shown that the resulting detonation speeds agree closely with the Chapman-Jouguet theoretical speed. That is, for this driver pressure ratio, the degree of overdrive should be very close to one (i.e., $f \approx 1.0$). However, for the high-resolution computations in the present study, the detonation wave at this driver pressure ratio contains very complex, irregular oscillations for the equivalence ratio range $0.6 < \phi < 1.0$. (The $\phi = 0.4$ case should be run for longer times to determine the oscillation pattern). This behavior for $p_0 = 0.4$ bar, and degree of overdrive close to one, agrees with the findings of Sussman[18] for a stoichiometric hydrogen-air mixture at nearly identical initial pressure and temperature. Bourlioux et al.[21] also showed that the oscillations obtained with a one-step chemistry model became nearly chaotic for low degrees of overdrive. It is not clear wether the one-dimensional detonations considered

here are inherently unstable at these conditions or wether further grid refinement is necessary to obtain accurate solutions.

Conclusions

The one-dimensional Euler equations with finite rate chemistry were solved to investigate the structure and stability of detonation waves for hydrogen-air mixtures at various equivalence ratios and pressures. The results indicate that the solutions to the governing equations do not include a steadily propagating detonation wave. Instead, the solutions always exhibit an unsteady oscillatory propagation mode. For mixtures close to stoichiometric conditions, the detonation wave propagates in a high-frequency low amplitude mode that is described by the McVey-Toong mechanism. For very lean mixtures, the detonation wave switches to a low-frequency, high-amplitude propagation mode similar to the "galloping" detonations observed experimentally in near-limit mixtures.

The transition from the high-frequency mode to the low-frequency mode depends on the degree of overdrive. High degrees of overdrive tend to stabilize the detonation wave and delay the transition to the low-frequency mode for lean mixtures. The frequency and amplitude of the oscillations are very uniform for high degrees of overdrive. At low pressures (p_0 = 0.2 bar), solutions that behave according to the McVey-Toong mechanism were possible for degrees of overdrive close to one. For higher pressures (p_0 > 0.4 bar), these solutions were possible only for degrees of overdrive above 1.07. Calculations with degrees of overdrive close to one at the higher pressures resulted in complex, irregular oscillations.

References

1. Schauer, F., Stutrud, J. and Bradley, R., "Detonation Initiation Studies and Performance Results for Pulsed Detonation Engine Applications," AIAA paper 2001-1129, Jan. 2001.

2. Povinelli, L.A. and Yungster, S., "Thermodynamic Cycle and CFD Analyses for Hydrogen Fueled Air-Breathing Pulse Detonation Engines," AIAA paper 2002-3629, July 2002.

3. Povinelli, L.A. and Yungster, S., "Airbreathing Pulse Detonation Engine Performance," NASA TM 2002-211575, also JANNAF Conference, 26th Airbreathing Propulsion Subcommittee, Destin, FL, April 2002.

4. Yungster, S. and Perkins, H.D., "Multiple- Cycle Simulation of a Pulse Detonation Engine Ejector," AIAA paper 2002-3630, July 2002.

5. Porter, J.L. and Squyers, R.A., "A Summary/Overview of Ejector Augmentor Theory and Performance," ATC Report No. R-91100/9CR-47A, Sept. 1979.

6. Gordon, W.E., Mooradian, A.J. and Harper, S.A., "Limit and Spin Effects in Hydrogen-Oxygen Detonations," *Seventh Symposium (Inter) on Combustion*, P752-759, Butterworths, 1959.

7. Dupre, G., Knystautas, R. and Lee, J.H., "Near-Limit Propagation of Detonation in Tubes," *10th International Colloquium on Dynamics of Explosions and Reactive Systems*, Berkeley, CA, Aug. 1985.

8. Belles, F.E., "Detonability and Chemical Kinetics: Prediction of Limits of Detonability of Hydrogen," *Seventh Symposium (Inter) on Combustion*, P745-751, Butterworths, 1959.

9. Dove, J.E. and Tribbeck, T.D., "Computational Study of the Kinetics of the Hydrogen-Oxygen Reaction Behind Steady State Shock Waves. Application to the Composition Limits and Transverse Stability of Gaseous Detonations," *Astronautica Acta*, Vol. 15 pp. 387-397, 1970.

10. Radhakrishnan, K., "Combustion Kinetics and Sensitivity Analysis Computations," in *Numerical Approaches to Combustion*, E.S. Oran and J.P. Boris, Eds., AIAA, Washington, DC, 1991, pp. 83-128.

11. Radhakrishnan, K., "LSENS–A General Chemical Kinetics and Sensitivity Analysis Code for Homogeneous Gas-Phase Reactions. I. Theory and Numerical Solution Procedures," NASA RP-1328, 1994.

12. McBride, B.J. and Gordon, S., "Computer Program for Calculation of Complex Chemical Equilibrium Compositions and Applications. II. Users Manual and Program Description," NASA RP-1311, 1996.

13. Jachimowski, C.J., "An Analytical Study of the Hydrogen-Air Reaction Mechanism with Application to Scramjet Combustion," NASA TP-2791, Feb. 1988.

14. Laffitte, P. F., "Flames of high-speed detonation," *Science of Petroleum*, Vol. IV, pp. 2995-3003, 1938.

15. Yungster, S., "Numerical Study of Shock-Wave Boundary Layer Interactions in Premixed Combustible Gases," *AIAA Journal*, Vol. 30, No. 10, 1992, pp. 2379-2387.

16. Yee, H.C., "Construction of Explicit and Implicit Symmetric TVD Schemes and Their Applications," *Journal of Computational Physics*, Vol. 68, 1987, pp. 151-179.

17. Yungster, S. and Radhakrishnan, K., "A Fully Implicit Time Accurate Method for Hypersonic Combustion: Application to Shock-Induced Combustion Instability," *Shock Waves*, Vol. 5, 1996, pp. 293-303.

18. Sussman, M.A., "A Computational Study of Unsteady Shock Induced Combustion of Hydrogen-Air Mixtures," AIAA paper 94-3101, June 1994.

19. Lehr, H.F., "Experiments on Shock-Induced Combustion," *Acta Astronautica*, Vol. 17, 1972, pp. 589-597.

20. McVey, J.B. and Toong, T.Y., "Mechanism of Instabilities of Exothermic Hypersonic Blunt Body Flows," *Combustion Science and Technology*, Vol. 3, pp. 63-76, 1971.

21. Bourlioux, A., Majda, A.J. and Roytburd, V., "Theoretical and Numerical Structure of Unstable One-Dimensional Detonations," *SIAM Journal of Applied Mathematics,* Vol. 51, pp. 303-343, April 1991.

TABLE 1.—H_2-Air Reaction Mechanism[a]

No.	Reaction	A	b	Θ
1	$H_2 + O_2 = HO_2 + H$	1.0×10^{14}	0.0	28197.38
2	$H + O_2 = OH + O$	2.6×10^{14}	0.0	8459.21
3	$H_2 + O = OH + H$	1.8×10^{10}	1.0	4481.37
4	$H_2 + OH = H + H_2O$	2.2×10^{13}	0.0	2593.15
5	$OH + OH = O + H_2O$	6.3×10^{12}	0.0	548.84
6[b]	$H + OH + M = H_2O + M$	2.2×10^{22}	-2.0	0.0
7[b]	$H + H + M = H_2 + M$	6.4×10^{17}	-1.0	0.0
8[b]	$H + O + M = OH + M$	6.0×10^{16}	-0.6	0.0
9[b]	$H + O_2 + M = HO_2 + M$	2.1×10^{15}	0.0	-503.52
10	$O + O + M = O_2 + M$	6.0×10^{13}	0.0	906.34
11	$HO_2 + H = OH + OH$	1.4×10^{14}	0.0	543.81
12	$HO_2 + H = H_2O + O$	1.0×10^{13}	0.0	543.81
13	$HO_2 + O = O_2 + OH$	1.5×10^{13}	0.0	478.35
14	$HO_2 + OH = H_2O + O_2$	8.0×10^{12}	0.0	0.0
15	$HO_2 + HO_2 = H_2O_2 + O_2$	2.0×10^{12}	0.0	0.0
16	$H + H_2O_2 = H_2 + HO_2$	1.4×10^{12}	0.0	1812.69
17	$O + H_2O_2 = OH + HO_2$	1.4×10^{13}	0.0	3222.56
18	$OH + H_2O_2 = H_2O + HO_2$	6.1×10^{12}	0.0	720.04
19[b]	$H_2O_2 + M = OH + OH + M$	1.2×10^{17}	0.0	22910.37

[a]Forward rate coefficient $k_f = AT^b \exp(-\Theta/T)$; units are moles, seconds, centimeters, and Kelvins.

[b]Third-body efficiencies:
Reaction 6: $H_2O = 6.0$; Reaction 7: $H_2O = 6.0$;
Reaction 8: $H_2O = 5.0$; Reaction 9: $H_2O = 16.0$, $H_2 = 2.0$;
Reaction 19: $H_2O = 15.0$.

TABLE 2.—Ignition Delay Time (t_{ig}) for $\phi=1.0$, $T_1=1250.0$ K

p_1 (bar)	t_{ig} (μs)
0.5	50.3
1.0	25.1
10.0	4.8
15.0	11.1
20.0	41.0
25.0	54.7
30.0	60.3
40.0	62.3
50.0	60.1
75.0	52.0
100.0	44.9
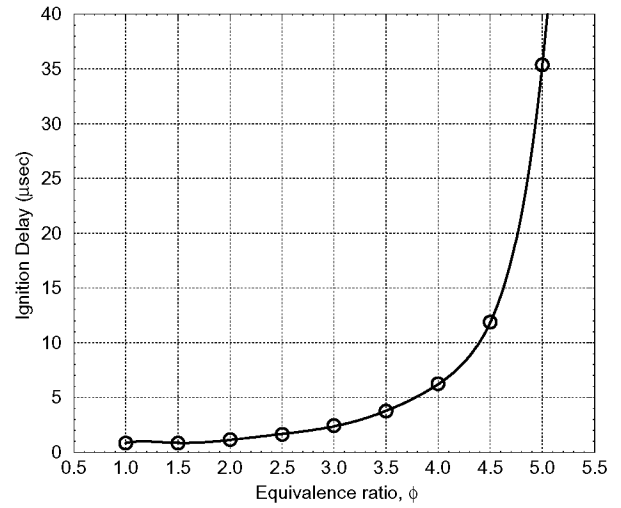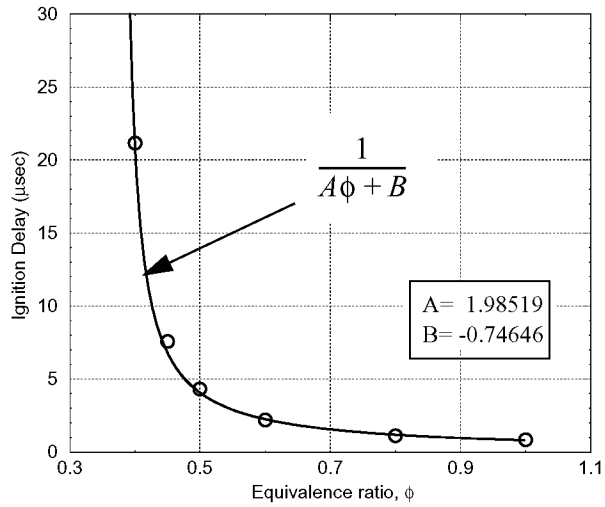
Fig. 1. Ignition delay for Chapman-Jouguet detonations in H_2-Air; p_0=0.4 bar, T_0=298 K.
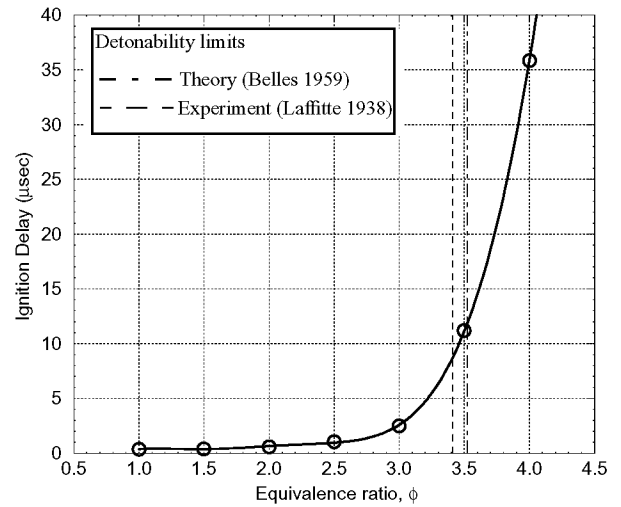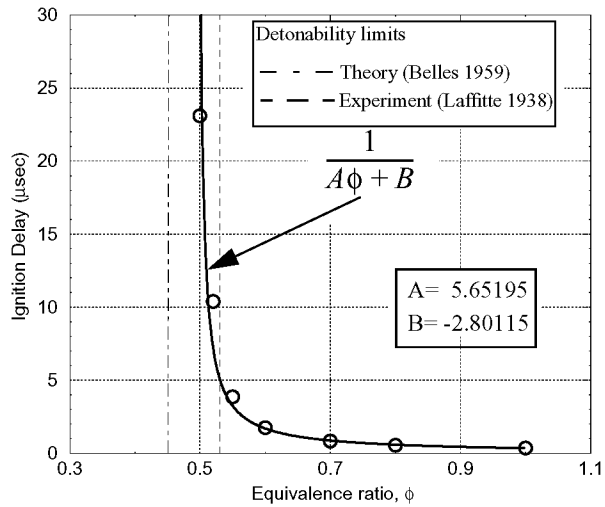
Fig. 2. Ignition delay for Chapman-Jouguet detonations in H_2-Air; p_0=1.0 bar, T_0=298 K.

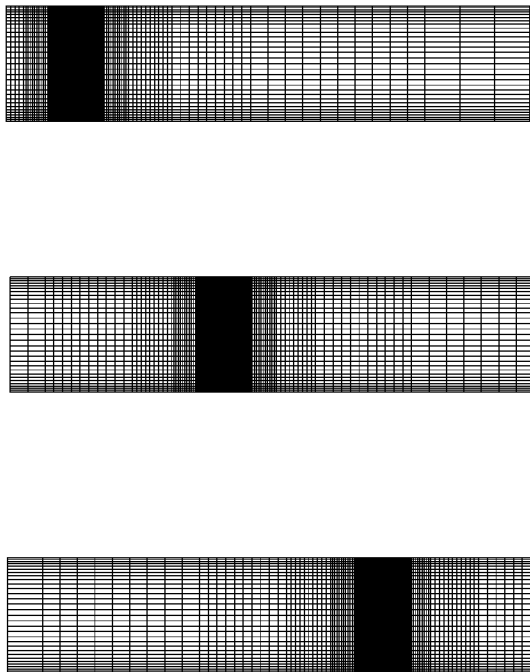Fig. 3. Computational grid at three different times.

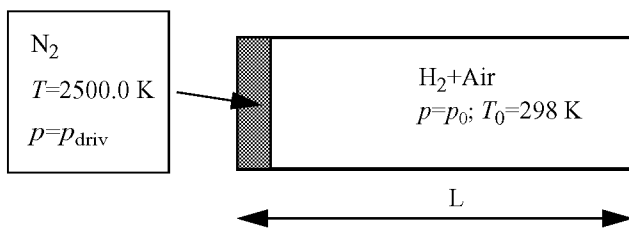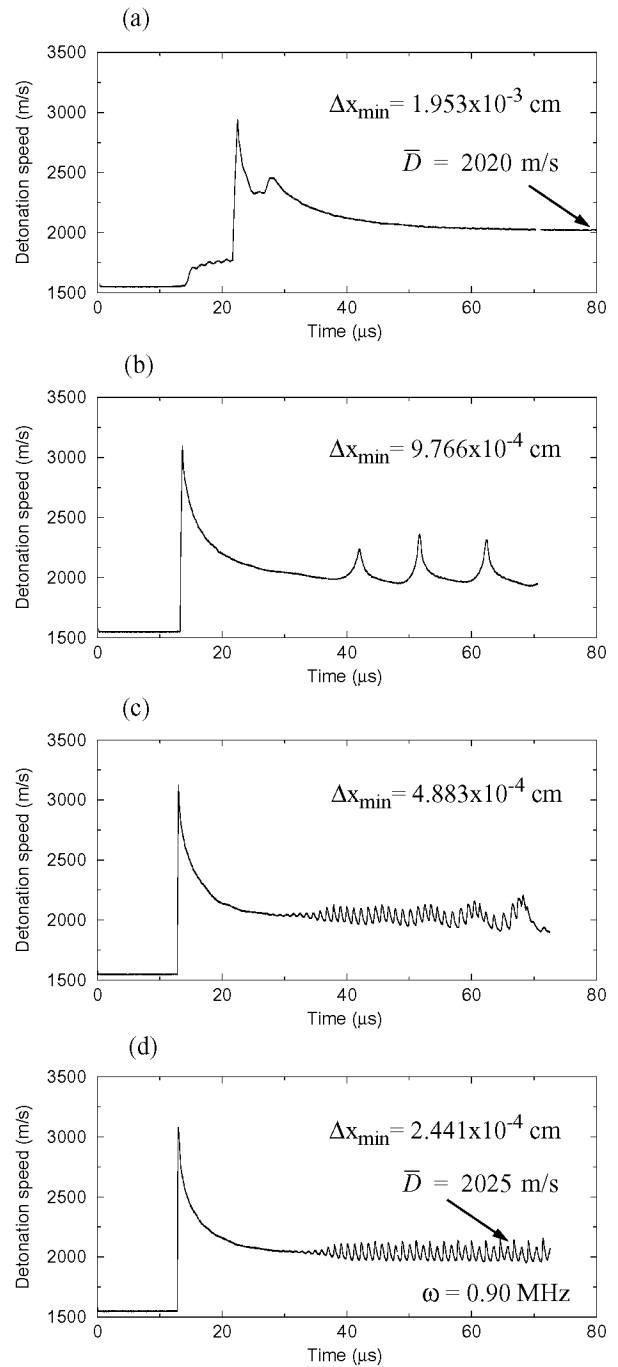Fig. 4. Schematic of detonation wave initiation.

(a)

$\Delta x_{min} = 1.953 \times 10^{-3}$ cm

$\overline{D} = 2020$ m/s

(b)

$\Delta x_{min} = 9.766 \times 10^{-4}$ cm

(c)

$\Delta x_{min} = 4.883 \times 10^{-4}$ cm

(d)

$\Delta x_{min} = 2.441 \times 10^{-4}$ cm

$\overline{D} = 2025$ m/s

$\omega = 0.90$ MHz

Fig. 5. Detonation speed as a function of time; H_2-Air; $p_0 = 0.4$ bar, $\phi = 1.0$; $r_p = p_{driv}/p_0 = 100$; $D_{CJ} = 1956.2$ m/s; f = 1.07.
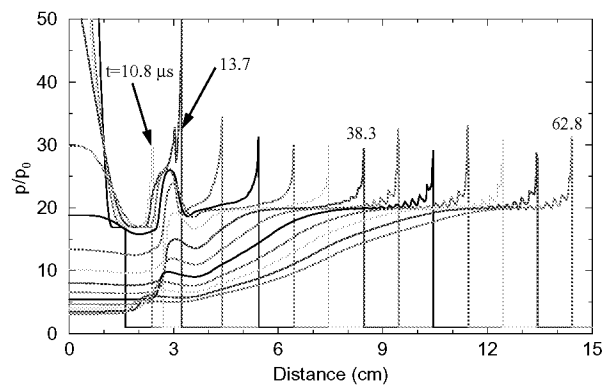
Fig. 6. Pressure ratio as a function of distance at different times; H_2-Air; $p_0 = 0.4$ bar, $\phi=1.0$; $r_p = p_{driv}/p_0 = 100$.
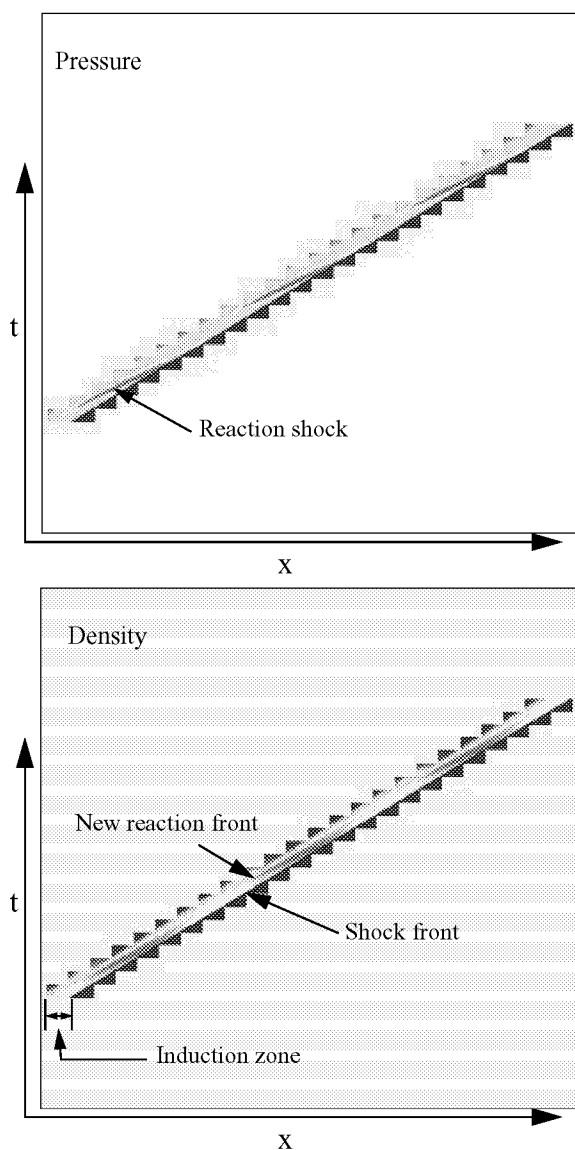
Fig. 7. History of pressure and density (x-t diagram) showing the Mcvey-Toong mechanism; $r_p=150$.
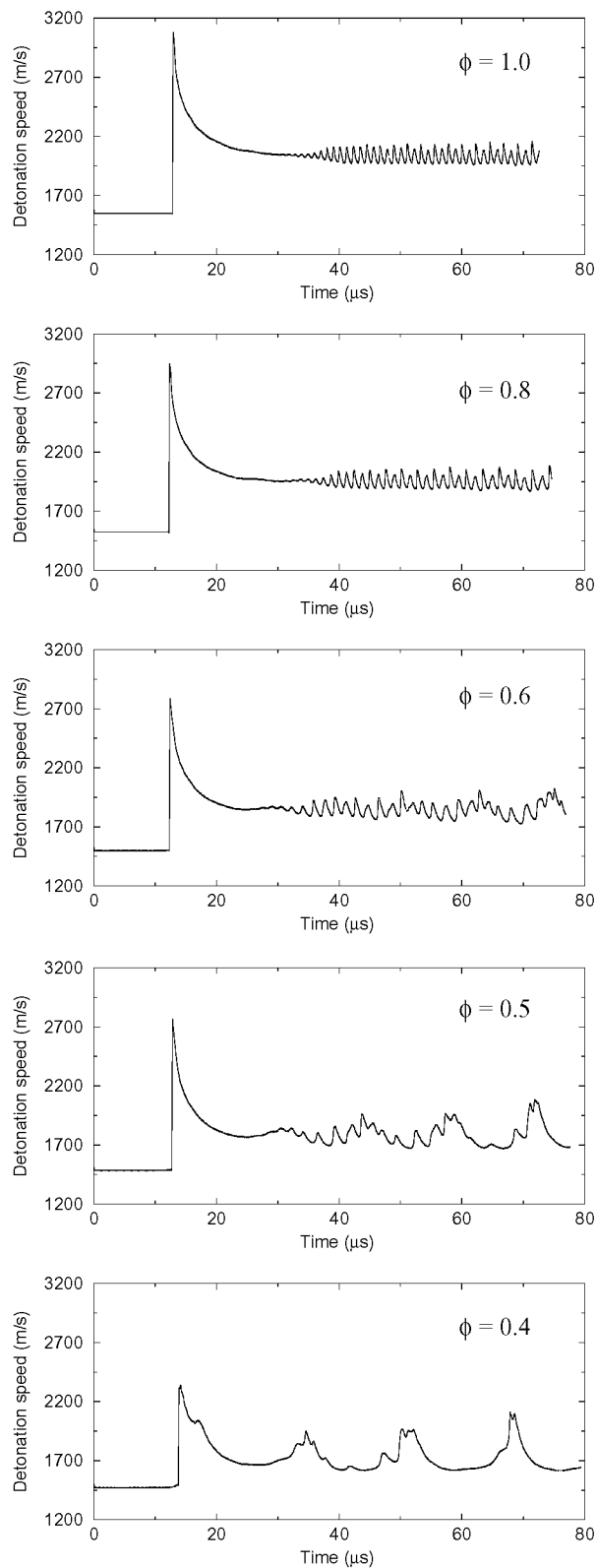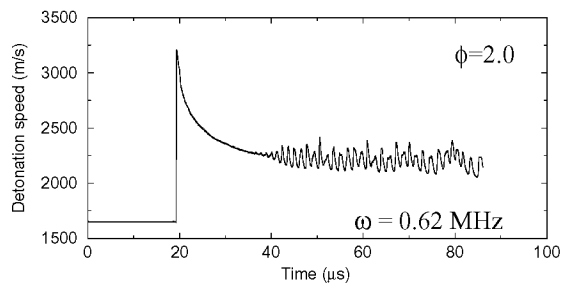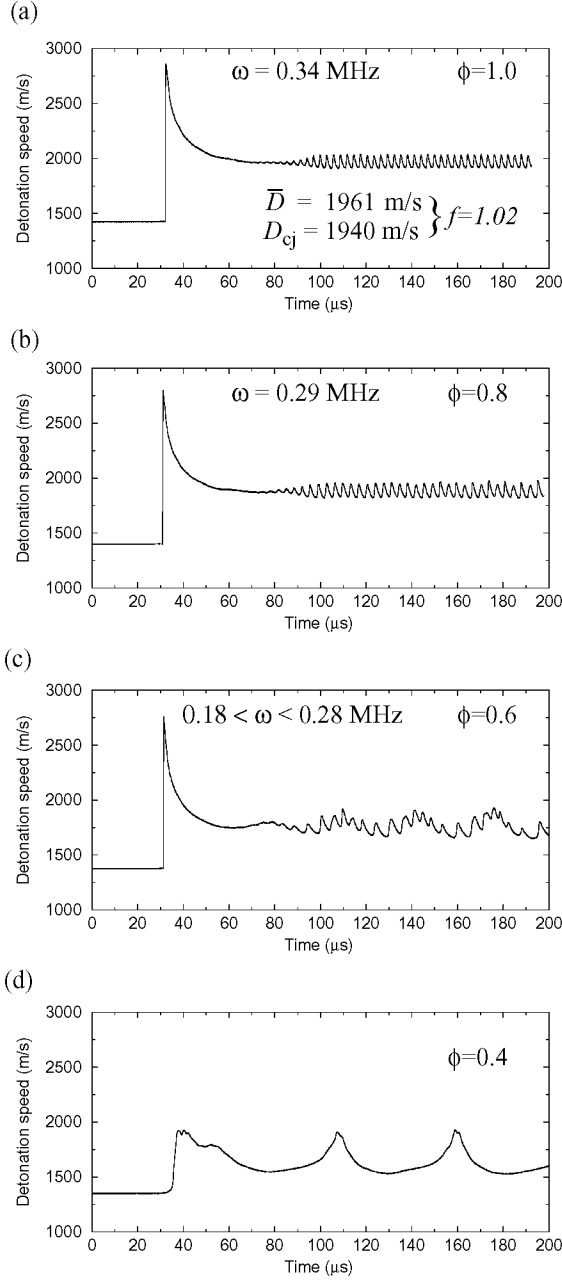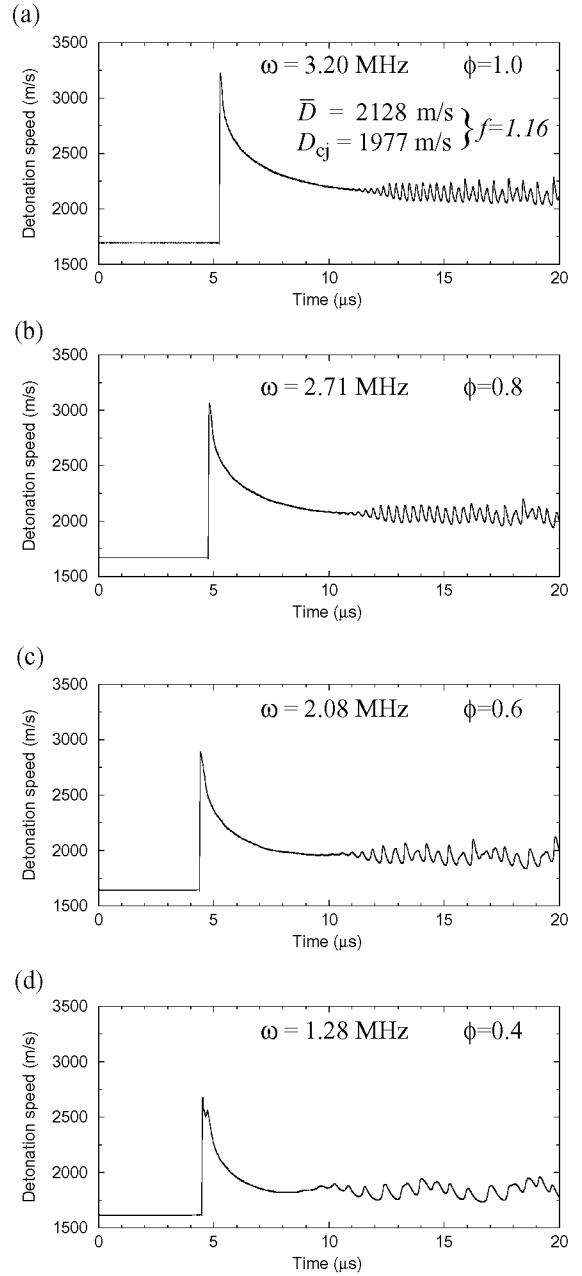

Fig. 8. Detonation speed as a function of time; H_2-Air; $p_0 = 0.4$ bar, $r_p = 100$, $\Delta x_{min}=2.441\times10^{-4}$ cm.
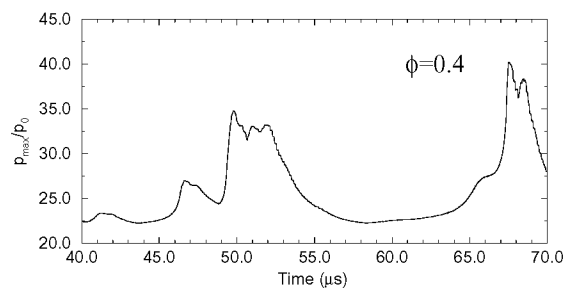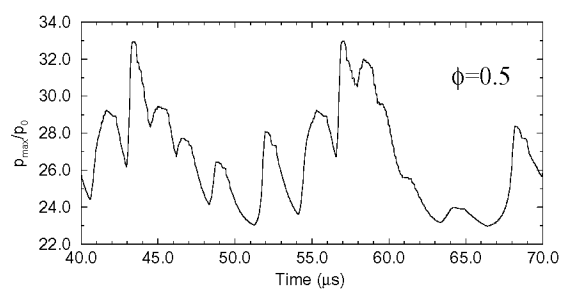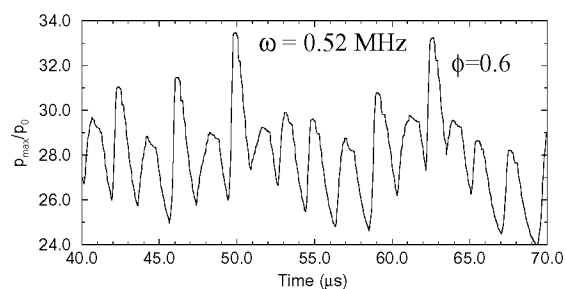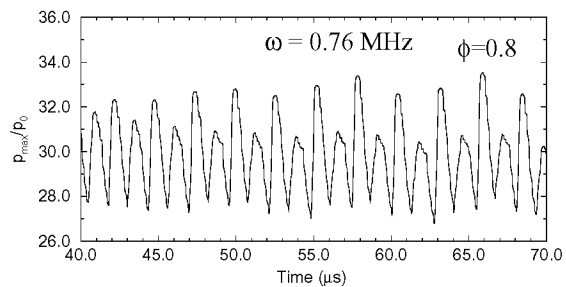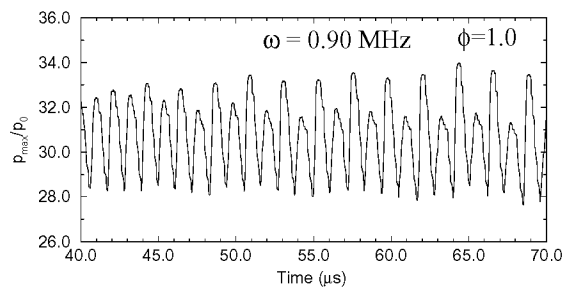
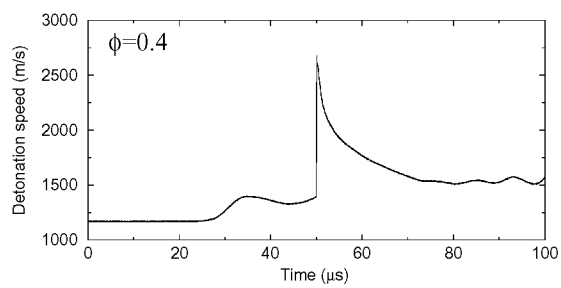Fig. 9. Maximum pressure as a function of time; H_2-Air; p_0 = 0.4 bar, r_p = 100, Δx_{min}=2.441x10^{-4} cm.
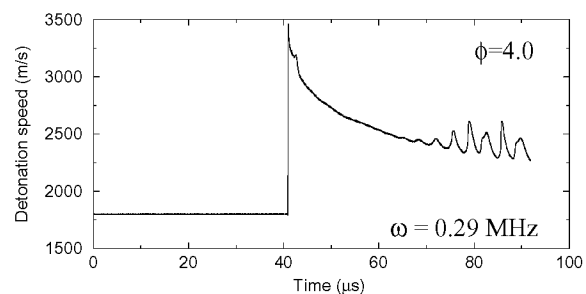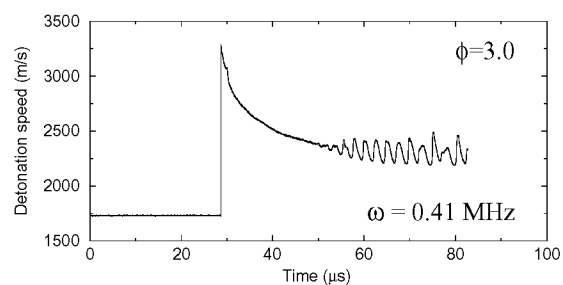
Fig. 10. Detonation speed as a function of time; H_2-Air; p_0 = 0.4 bar, r_p = 100, Δx_{min}=2.441x10^{-4} cm.

(a)

(b)

(c)

(d)

(a)

(b)

(c)

(d)

Fig. 11. Detonation speed as a function of time; H_2-Air; $p_0 = 0.2$ bar, $r_p = 70$, $\Delta x_{min} = 2.441 \times 10^{-4}$ cm.

Fig. 12. Detonation speed as a function of time; H_2-Air; $p_0 = 1.0$ bar, $r_p = 150$, $\Delta x_{min} = 7.324 \times 10^{-5}$ cm.
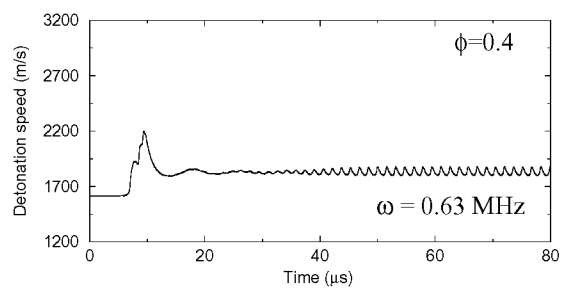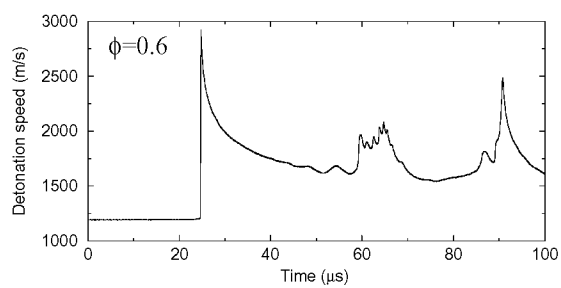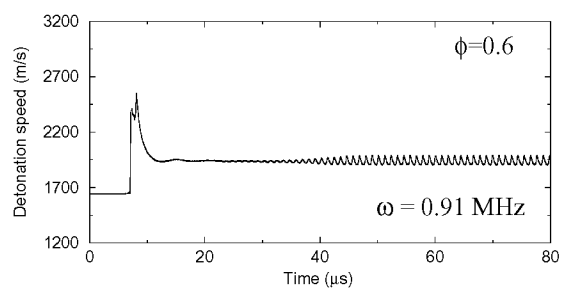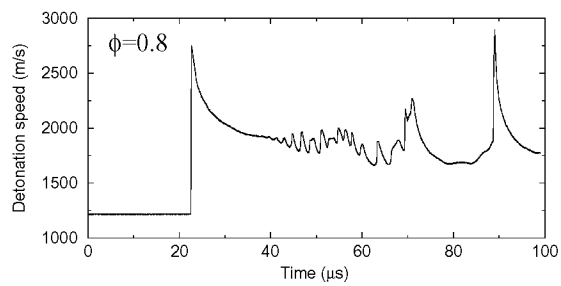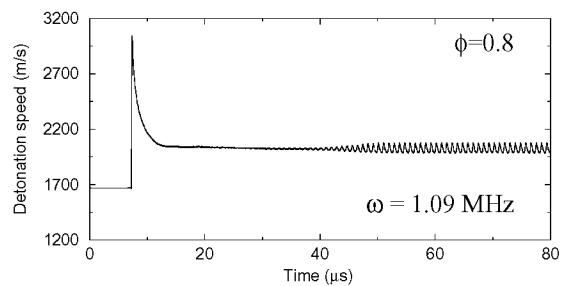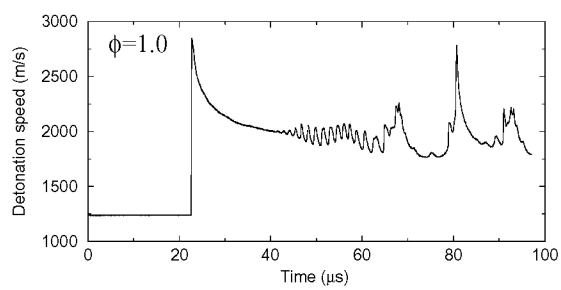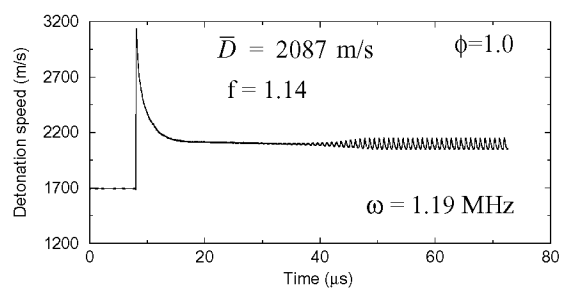
Fig. 13. Detonation speed as a function of time; H_2-Air; $p_0 = 0.4$ bar, $r_p = 150$, $\Delta x_{min} = 2.441 \times 10^{-4}$ cm.

Fig. 14. Detonation speed as a function of time; H_2-Air; $p_0 = 0.4$ bar, $r_p = 40$, $\Delta x_{min} = 2.441 \times 10^{-4}$ cm.

REPORT DOCUMENTATION PAGE

Public reporting burden for this collection of information is estimated to average 1 hour per response, including the time for reviewing instructions, searching existing data sources, gathering and maintaining the data needed, and completing and reviewing the collection of information. Send comments regarding this burden estimate or any other aspect of this collection of information, including suggestions for reducing this burden, to Washington Headquarters Services, Directorate for Information Operations and Reports, 1215 Jefferson Davis Highway, Suite 1204, Arlington, VA 22202-4302, and to the Office of Management and Budget, Paperwork Reduction Project (0704-0188), Washington, DC 20503.

1. AGENCY USE ONLY (Leave blank)	2. REPORT DATE October 2002	3. REPORT TYPE AND DATES COVERED Contractor Report

4. TITLE AND SUBTITLE

Computational Study of Near-Limit Propagation of Detonation in Hydrogen-Air Mixtures

6. AUTHOR(S)

S. Yungster and K. Radhakrishnan

5. FUNDING NUMBERS

WU–708–48–13–00
NCC3–542

7. PERFORMING ORGANIZATION NAME(S) AND ADDRESS(ES)

Institute for Computational Mechanics in Propulsion
22800 Cedar Point Road
Brook Park, Ohio 44142

8. PERFORMING ORGANIZATION REPORT NUMBER

E–13571

9. SPONSORING/MONITORING AGENCY NAME(S) AND ADDRESS(ES)

National Aeronautics and Space Administration
Washington, DC 20546–0001

10. SPONSORING/MONITORING AGENCY REPORT NUMBER

NASA CR—2002-211889
ICOMP–2002–06
AIAA–2002–3712

11. SUPPLEMENTARY NOTES

Prepared for the 38th Propulsion Conference and Exhibit, cosponsored by the AIAA, ASME, SAE, and ASEE, Indianapolis, Indiana, July 7–10, 2002. Project Manager, Charles Trefney, Turbomachinery and Propulsion Systems Division, NASA Glenn Research Center, organization code 5880, 216–433–2162.

12a. DISTRIBUTION/AVAILABILITY STATEMENT

Unclassified - Unlimited
Subject Category: 34   Distribution: Nonstandard

Available electronically at http://gltrs.grc.nasa.gov

This publication is available from the NASA Center for AeroSpace Information, 301–621–0390.

12b. DISTRIBUTION CODE

13. ABSTRACT (Maximum 200 words)

A computational investigation of the near-limit propagation of detonation in lean and rich hydrogen-air mixtures is presented. The calculations were carried out over an equivalence ratio range of 0.4 to 5.0, pressures ranging from 0.2 bar to 1.0 bar and ambient initial temperature. The computations involved solution of the one-dimensional Euler equations with detailed finite-rate chemistry. The numerical method is based on a second-order spatially accurate total-variation-diminishing (TVD) scheme, and a point implicit, first-order-accurate, time marching algorithm. The hydrogen-air combustion was modeled with a 9-species, 19-step reaction mechanism. A multi-level, dynamically adaptive grid was utilized in order to resolve the structure of the detonation. The results of the computations indicate that when hydrogen concentrations are reduced below certain levels, the detonation wave switches from a high-frequency, low amplitude oscillation mode to a low frequency mode exhibiting large fluctuations in the detonation wave speed; that is, a "galloping" propagation mode is established.

14. SUBJECT TERMS

Unstable detonations; Detonability limits; Computational fluid dynamics

15. NUMBER OF PAGES
18

16. PRICE CODE

17. SECURITY CLASSIFICATION OF REPORT Unclassified	18. SECURITY CLASSIFICATION OF THIS PAGE Unclassified	19. SECURITY CLASSIFICATION OF ABSTRACT Unclassified	20. LIMITATION OF ABSTRACT

NSN 7540-01-280-5500

Standard Form 298 (Rev. 2-89)
Prescribed by ANSI Std. Z39-18
298-102